IAI Journals.ASM.org

Gastric *De Novo* Muc13 Expression and Spasmolytic Polypeptide-Expressing Metaplasia during *Helicobacter heilmannii* Infection

Cheng Liu,[a] Annemieke Smet,[a] Caroline Blaecher,[a] Bram Flahou,[a] Richard Ducatelle,[a] Sara Linden,[b] Freddy Haesebrouck[a]

Department of Pathology, Bacteriology and Avian Diseases, Faculty of Veterinary Medicine, Ghent University, Merelbeke, Belgium[a]; Mucosal Immunobiology and Vaccine Center, Sahlgrenska Academy, Gothenburg University, Gothenburg, Sweden[b]

***Helicobacter heilmannii* is a zoonotic bacterium that has been associated with gastric disease in humans. In this study, the mRNA expression of mucins in the stomach of BALB/c mice was analyzed at several time points during a 1-year infection with this bacterium, during which gastric disease progressed in severity. Markers for acid production by parietal cells and mucous metaplasia were also examined. In the first 9 weeks postinfection, the mRNA expression of Muc6 was clearly upregulated in both the antrum and fundus of the stomach of *H. heilmannii*-infected mice. Interestingly, Muc13 was upregulated already at 1 day postinfection in the fundus of the stomach. Its expression level remained high in the stomach over the course of the infection. This mucin is, however, not expressed in a healthy stomach, and high expression of this mucin has so far only been described in gastric cancer. In the later stages of infection, mRNA expression of H^+/K^+-ATPase α/β and KCNQ1 decreased, whereas the expression of Muc4, Tff2, Dmbt1, and polymeric immunoglobulin receptor (pIgR) increased starting at 16 weeks postinfection onwards, suggesting the existence of spasmolytic polypeptide-expressing metaplasia in the fundus of the stomach. Mucous metaplasia present in the mucosa surrounding low-grade mucosa-associated lymphoid tissue (MALT) lymphoma-like lesions was also histologically confirmed. Our findings indicate that *H. heilmannii* infection causes severe gastric pathologies and alterations in the expression pattern of gastric mucins, such as Muc6 and Muc13, as well as disrupting gastric homeostasis by inducing the loss of parietal cells, resulting in the development of mucous metaplasia.**

Helicobacter pylori is the major predisposing factor for the development of chronic active gastritis, peptic ulcers, and gastric adenocarcinomas in humans, and approximately 15% of infected individuals are estimated to develop such symptoms. This pathogen can be detected attached to gastric epithelial cells but is found mainly within the mucus layer and is able to bind to highly glycosylated mucins. MUC1, MUC5AC, and MUC6 are the major mucins covering the healthy gastric mucosa. The membrane-associated MUC1 and secreted MUC5AC are expressed at the surface epithelium, whereas MUC6 is secreted by glandular cells (1–4).

H. pylori infection causes alterations in the expression pattern, glycosylation, and distribution of gastric mucins, as well as disrupting the gastric homeostasis by inducing the loss of parietal cells (5, 6). The loss of parietal cells can lead to two distinct types of mucous metaplasia: intestinal metaplasia and spasmolytic polypeptide-expressing metaplasia (SPEM). It has been suggested that intestinal metaplasia develops in the presence of pre-existing SPEM, supporting the role of SPEM as a neoplastic precursor in the carcinogenesis cascade (6). The intestinal mucins MUC2, MUC4, and MUC13 are not expressed in the healthy gastric mucosa but have been detected in gastric adenocarcinomas and during stages of mucous metaplasia (7–9).

Besides *H. pylori*, other spiral-shaped non-*H. pylori Helicobacter* spp. (NHPH), such as *H. suis* in pigs and *H. heilmannii* (*sensu stricto*), *H. felis*, *H. bizzozeronii*, and *H. salomonis* in cats and dogs, have been associated with gastric disease in humans (10, 11). *H. heilmannii* is highly prevalent in healthy cats and dogs, as well as in animals with chronic gastritis (10). In humans, this *Helicobacter* species has been associated with gastritis, gastric and duodenal ulcers, and low-grade mucosa-associated lymphoid tissue (MALT) lymphoma. It has been detected in 8 to 19% of gastric biopsy specimens with histological evidence of NHPH infection (10–12). Living in close contact with cats and dogs has been identified as a significant risk factor for these infections in humans (10). Since this species has only recently been isolated and cultured *in vitro*, information on how *H. heilmannii* interacts with the human stomach and causes disease still remains poor. Comparative genomic analyses showed that although the *H. heilmannii* genome contains several genes encoding homologues of known *H. pylori* virulence factors, it lacks a Cag pathogenicity island (Cag-PAI), as well as genes encoding the vacuolating cytotoxin VacA and several outer membrane proteins involved in the binding of *H. pylori* to the gastric mucosa, such as BabA/-B, SabA, AlpA/-B, OipA, HopZ, HopQ, and HomB (13). Thus, factors that contribute to the colonization properties of *H. heilmannii*, particularly adhesion, remain to be identified. A recent infection study in a Mongolian gerbil model for human *Helicobacter*-induced pathology showed variations in colonization capacity and virulence between different *H. heilmannii* strains isolated from the gastric mucosa of cats. These findings are most probably also relevant for infection with this bacterium in humans (14). Unlike *H. pylori*, which is mainly observed at the surface epithelium and close to MUC1- and MUC5AC-producing cells (1, 3), *H. heilmannii* is mostly found in the gastric pits, as has also been described for

Received 2 April 2014 **Accepted** 12 May 2014
Published ahead of print 27 May 2014
Editor: S. R. Blanke
Address correspondence to Annemieke Smet, Annemieke.Smet@Ugent.be.
C.L. and A.S. share first authorship. S.L. and F.H. share senior authorship.
Supplemental material for this article may be found at http://dx.doi.org/10.1128/IAI.01867-14.

doi:10.1128/IAI.01867-14

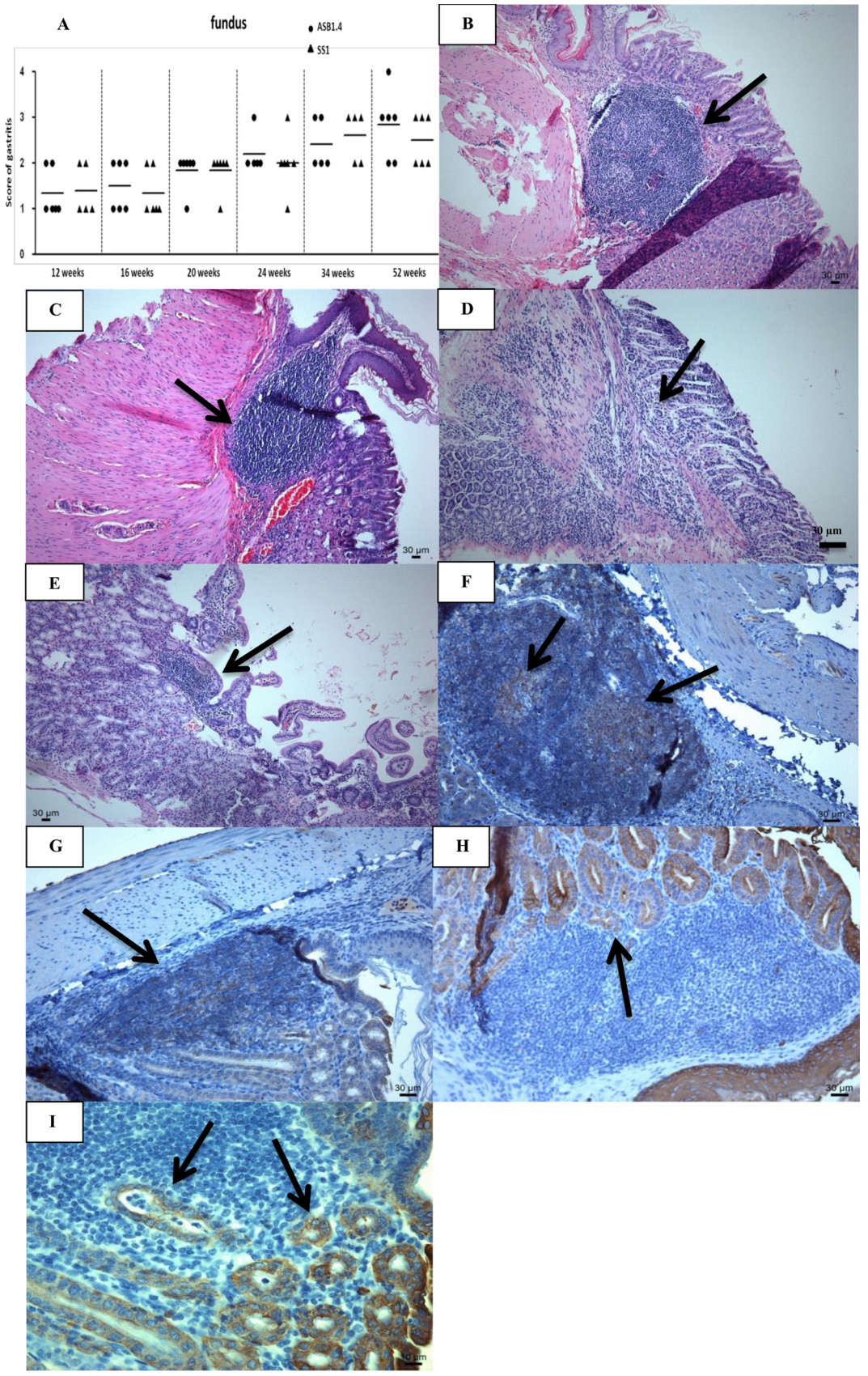
A
fundus
ASB1.4
SS1
Score of gastritis
0
1
2
3
4
12 weeks
16 weeks
20 weeks
24 weeks
34 weeks
52 weeks
B
C
D
E
F
G
H
I
30 μm

other NHPH (14, 15). This bacterium can be found in close association with parietal cells but is also able to bind to human mucus-secreting epithelial cells, as well as to mucin samples containing highly glycosylated MUC5AC and MUC6 (unpublished data). Whether an *H. heilmannii* infection has an impact on the distribution and expression of the gastric MUC1, MUC5AC, and MUC6 mucins is currently unknown.

Specific-pathogen-free (SPF) inbred C57BL/6 and BALB/c mice have been shown to be useful models for the study of *Helicobacter*-related human gastric disease (15). C57BL/6 mice have been described genetically as predominant Th1 responders, while BALB/c mice are mainly Th2 responders (15). It has been shown that infection with *H. suis* induces a predominant Th17/Th2 immune response in BALB/c mice and even in C57BL/6 mice in the absence of a Th1 response, but with a more pronounced inflammation in BALB/c mice (16). More recently, it has been suggested that infection with *H. heilmannii* also elicits a Th2 immune response (14). These results are in contrast to the predominant Th17/Th1 response mostly seen during *H. pylori* infection in mice (16). Therefore, in the present study, we used Th2-prone BALB/c mice to investigate the expression levels of Muc1, Muc5ac, and Muc6 in the stomach at several time points during a 1-year *H. heilmannii* infection during which gastric disease progressed from gastritis to MALT lymphoma-like lesions and mucous metaplasia. Since *H. heilmannii* has been found close to parietal cells in the gastric pits, markers for acid production by parietal cells were examined. Markers for mucous metaplasia (in particular the Muc2, Muc4, and Muc13 intestinal mucins) as a result of parietal cell loss were included as well. Infection with the mouse-adapted *H. pylori* SS1, a strain that elicits a Th2 response, was included for comparison (16).

MATERIALS AND METHODS

Animals. Six-week-old female SPF BALB/c mice were purchased from Harlan NL (Horst, The Netherlands). The animals were housed in individual filter-top cages, had free access to water and food (an autoclaved commercial diet, Teklad 2018S, containing 18% protein; Harlan) throughout the experiment, and were monitored daily.

The *in vivo* experimental protocol was approved by the Ethical Committee of the Faculty of Veterinary Medicine, Ghent University, Belgium (EC 2011-155, 27 October 2011).

Cultivation of *H. heilmannii* and *H. pylori* strains used for infection. The highly virulent *H. heilmannii* strain ASB1.4, isolated from the stomach of a kitten with gastritis, was cultivated as described previously (11, 14). After incubation under microaerobic conditions (11), the bacteria were harvested, and the final concentration was adjusted to 7×10^8 viable bacteria/ml.

The mouse-adapted *H. pylori* SS1 strain (17) was grown for 3 days on blood agar plates (Oxoid) and further cultured overnight in brucella broth (Oxoid) under microaerobic conditions. The optical density was then adjusted to 1.5, corresponding to approximately 1×10^9 viable bacteria/ml.

Experimental procedure. For each time point tested, 6 animals were intragastrically inoculated 3 times at 2-day intervals with 300 μl of an ASB1.4 or SS1 bacterial suspension and 3 animals were inoculated with brucella broth (pH 5) as a negative control. Inoculation was performed under brief isoflurane anesthesia (2.5%), using a feeding needle. At 1 day, 4 days, and 1, 2, 3, 4, 9, 12, 16, 20, 24, 34, and 52 weeks after the first inoculation, the animals were euthanized by cervical dislocation under deep isoflurane anesthesia (5%). The stomach and the duodenum of each mouse were resected, and samples were taken for histopathological examination and quantitative real-time (RT)-PCR analysis.

Histopathology and immunohistochemistry. A longitudinal section, starting from the end of the forestomach and comprising the antrum and the fundus of the stomach and part of the duodenum, was fixed in 10% phosphate-buffered formalin and embedded in paraffin for light microscopy. From each animal, several consecutive paraffin slides of 5 μm were cut, deparaffinized, and dehydrated. Heat-induced antigen retrieval (100°C for 20 min) was then performed in citrate buffer (pH 6), and endogenous peroxidase activity and nonspecific reactions were blocked by incubating the slides with 3% H_2O_2 in methanol (5 min) and 30% goat serum (30 min), respectively. A hematoxylin and eosin (H&E) staining was performed on a first slide to score the intensity of the gastritis according to the updated Sydney system, as described previously (15) but with some modifications, as described in the legend to Fig. 1. On a second slide, B lymphocytes were visualized by immunohistochemical staining using a polyclonal rabbit anti-CD20 antibody (1/100; Thermo Scientific, Fremont, CA). On a third slide, parietal cells were identified by immunohistochemical staining using a mouse monoclonal antibody against the hydrogen potassium ATPase (1/200; Abcam Ltd., Cambridge, United Kingdom).

Muc13 expression was evaluated by immunohistochemical staining (one slide for each staining) using an anti-Muc13 antibody. Incubation with primary antibodies directed against CD20 and Muc13 was followed by incubation with a biotinylated goat anti-rabbit IgG antibody (1/500; DakoCytomation, Heverlee, Belgium). Incubation with primary antibody against the hydrogen potassium ATPase was followed by incubation with a biotinylated goat anti-mouse IgG antibody (1/200; DakoCytomation). After rinsing, the sections were incubated with a streptavidin-biotin-horseradish peroxidase complex (DakoCytomation), and the color was developed with diaminobenzidine tetrahydrochloride (DAB) and H_2O_2.

To highlight lymphoepithelial lesions, paraffin slides were stained with a monoclonal mouse anticytokeratin antibody (1/50; DakoCytomation) and further processed using an EnVision+ system for use with mouse primary antibodies (DakoCytomation).

Finally, periodic acid-Schiff stain (PAS)-Alcian blue staining was performed for the differential staining of glycoproteins.

DNA extraction and quantification of colonizing *Helicobacter* spp. in the stomach and duodenum. Samples from the fundus and the antrum of the stomach and from the duodenum of each animal were harvested into 1 ml RNAlater (Ambion, Austin, TX, USA) and stored at −70°C until RNA and DNA extraction. The tissue samples were then homogenized (MagNALyser; Roche, Mannheim, Germany), and RNA and DNA were

FIG 1 Gastric inflammation in *H. heilmannii*- and *H. pylori*-infected BALB/c mice. (A) Fundic inflammation was scored on a scale of 0 to 4, as follows: 0, no infiltration with mononuclear and/or polymorphonuclear cells; 1, mild diffuse infiltration with mononuclear and/or polymorphonuclear cells or the presence of one small (50 to 200 cells) aggregate of inflammatory cells; 2, moderate diffuse infiltration with mononuclear and/or polymorphonuclear cells and/or the presence of 2 to 4 inflammatory aggregates; 3, marked diffuse infiltration with mononuclear and/or polymorphonuclear cells and/or the presence of at least five inflammatory aggregates; 4, diffuse infiltration of large regions with large aggregates of mononuclear and/or polymorphonuclear cells. Results for individual animals are depicted by symbols around the means (lines). (B to E) H&E staining of the fundus, antrum, and duodenum of a *Helicobacter*-infected BALB/c mouse. (B and C) A large infiltrate of mononuclear cells (arrow) at the forestomach/stomach transition zone of a mouse infected with *H. heilmannii* ASB1.4 (B) and *H. pylori* SS1 (C) at 52 weeks postinfection. Bar = 30 μm. (D and E) A mild lymphocytic infiltration of the lamina muscularis mucosae in the antrum (D) and duodenum (E) of a mouse infected with *H. heilmannii* ASB1.4 for 52 weeks (arrows). Bar = 30 μm. (F and G) CD20 staining of the forestomach/stomach transition zone of a mouse infected with *H. heilmannii* ASB1.4 (F) and *H. pylori* SS1 (G) at 52 weeks postinfection, showing B lymphocytes (brown) in germinal centers of lymphoid follicles (arrows). Bar = 30 μm. (H and I) Cytokeratin staining of the forestomach/stomach transition zone of a mouse infected with *H. heilmannii* ASB1.4 (bar = 30 μm) (H) and *H. pylori* SS1 (bar = 10 μm) (I) at 52 weeks postinfection showing numerous lymphoepithelial lesions (arrows).

separated (14). The numbers of colonizing *H. heilmannii* and *H. pylori* bacteria per mg of gastric tissue were determined in the DNA samples using quantitative RT-PCRs specific for the detection of *H. heilmannii* and *H. pylori* (14, 16). *Helicobacter* standards were generated as described previously (18). One microliter of DNA template was suspended in a 10-μl reaction mixture consisting of 3.5 μl high-performance liquid chromatography (HPLC)-grade water, 5 μl SensiMix SYBR No-ROX (Bioline Reagents Ltd., United Kingdom), and 0.25 μl both primers (see Table S1 in the supplemental material) (Integrated DNA Technologies). Standards and DNA samples were run in duplicate on a CFX96 RT-PCR system with a C1000 thermal cycler (Bio-Rad, Hercules, CA, USA). For quantification of *H. heilmannii* and *H. pylori* DNA in the tissue samples, the Bio-Rad CFX Manager (version 1.6) software was used.

RT-PCR for gene expression. The total RNA concentration in each sample was utilized for first-strand cDNA synthesis using the iScript cDNA synthesis kit (Bio-Rad). Quantitative RT-PCR was carried out for measuring the gene expression levels of murine gastric mucins (Muc1, Muc2, Muc4, Muc5AC, Muc5B, Muc6, and Muc13), trefoil factors (Tff1 and Tff2), and Dmbt1, polymeric immunoglobulin receptor (pIgR), H^+/K^+-ATPase, Kcnq1, and Ckb. The housekeeping genes *PPIa*, *H2afz*, and *HPRT* were included as reference genes. The primer sequences are shown in Table S1 in the supplemental material. Reactions were performed in 10-μl volumes containing 1 μl cDNA, 0.05 μl both primers (see Table S1), 3.9 μl HPLC-grade water, and 5 μl SensiMix SYBR No-ROX. The experimental protocol for PCR (40 cycles) was performed on a CFX96 RT-PCR system with a C1000 thermal cycler (Bio-Rad). Control reactions without the reverse transcriptase step were implemented to exclude DNA contamination of the RNA samples. No-template control reaction mixtures were included, and all samples were run in duplicate. The results are shown as fold changes of mRNA expression in infected animals relative to the mRNA expression levels in control animals. Fold changes were calculated using the cycle threshold ($\Delta\Delta C_T$) method (19), with the mean C_T values from three uninfected mice as a control. Fold changes of ≥4 were accepted as upregulation and of ≤0.25 as downregulation.

Statistical analysis. Statistical analysis was performed using the SPSS Statistics 21 software package (IBM). Gastritis scores were analyzed using the nonparametric Mann-Whitney *U* test to compare groups. Gene expression was compared between different infected groups and controls using a Bonferroni *post hoc* test (analysis of variance [ANOVA]). For correlation between different variables, Spearman's rho correlation coefficients were calculated. Differences were considered statistically significant at a *P* value of ≤0.05.

RESULTS

Induction of inflammation by and colonization capacity of *H. heilmannii* ASB1 and *H. pylori* SS1. Gastric lymphoid lesions were not present in any of the noninfected control animals. For all of these animals, the histomorphology was considered to be normal, with only minor inflammatory cell infiltration in the gastric mucosa. Inflammation in *H. heilmannii* ASB1.4- and *H. pylori* SS1-infected mice was characterized by mononuclear and polymorphonuclear cell infiltration in the lamina propria mucosae, the tunica submucosa, or both, depending on the individual animal. At all time points, inflammation was observed mainly in the fundus. The fundic inflammation scores of each individual animal are shown in Fig. 1A. No statistically significant difference between inflammation scores for mice inoculated with ASB1.4 or SS1 at a certain time point was demonstrated. From 24 weeks postinfection onwards, large lymphoid aggregates of mononuclear and/or polymorphonuclear cells were mainly seen in a narrow zone in the fundus near the forestomach/stomach transition zone (Fig. 1B and C) of both *H. heilmannii*- and *H. pylori*-infected mice. In mice infected with ASB1.4 and SS1 for at least 34 weeks, B-cell-containing germinal centers were seen in those large lymphoid aggregates (Fig. 1F and G). In several mice infected with ASB1.4 and SS1 for 52 weeks, numerous lymphoepithelial MALT lymphoma-like lesions could be detected in the gastric mucosa (Fig. 1H and I). These were most abundant in a narrow zone in the fundus near the forestomach/stomach transition zone. In all *Helicobacter*-infected mice, mild signs of inflammation were detected in the antrum of the stomach and the duodenum at 52 weeks postinfection (Fig. 1D and E). However, inflammation could also be noted in the junction between antrum and fundus of mice infected with *H. heilmannii* for 52 weeks (data not shown).

Throughout the experiment, all control animals were negative for *Helicobacter* DNA in quantitative RT-PCR assays. At all time points, *Helicobacter* DNA was found in both the antrum and fundus of the stomach from all infected animals but with a larger amount in the antrum. *H. pylori* and *H. heilmannii* DNA was found in the duodenum from 3 and 12 weeks postinfection onwards, respectively (Fig. 2A, B, and C). In general, ASB1.4 colonized the stomach of mice at a significantly higher level than SS1 ($P = 0.002$ for antrum at 4, 20, 24, and 34 weeks postinfection; $P = 0.004$ for antrum at 12, 16, and 52 weeks postinfection; $P = 0.026$ for antrum at 9 weeks postinfection; $P = 0.009$ for fundus at 12 weeks postinfection; and $P = 0.002$ for fundus at 16, 20, 24, and 34 weeks postinfection). The amounts of ASB1.4 and SS1 DNA were much lower in the duodenum than in the stomach, and a significant difference between *H. heilmannii* and *H. pylori* was only seen at 3 weeks postinfection ($P = 0.015$) (Fig. 2C).

Changes in Muc1, Muc5AC, Muc5B, and Muc6 expression during *H. heilmannii* colonization. No change in mRNA expression of Muc1 and Muc5AC was seen in the stomach during the whole experiment (data not shown). In the first 9 weeks postinfection, quantitative RT-PCR showed clear upregulation in the mRNA expression of Muc6 in both the antrum (fold change for ASB1.4, 7.43 ± 2.08, and for SS1, 6.39 ± 2.5) and fundus (fold change for ASB1.4, 5.88 ± 2.66, and for SS1, 6.86 ± 3.01) of *Helicobacter*-infected mice compared to the expression in the control group (Fig. 3A and B; see also Fig. S1A and B in the supplemental material). In addition, a significant positive correlation was observed between Muc6 expression and *Helicobacter* colonization in the antrum of ASB1.4-infected mice (Fig. 3C).

Also in this early stage of infection, Muc5B was abnormally expressed in the stomach of mice infected with both species (Fig. 4A and B; see also Fig. S1C and D in the supplemental material). This mucin is normally not expressed in a healthy stomach (20). Compared to the results for the control animals, whose mRNA expression levels were set to 1, the fold differences in Muc5B and Muc5AC expression in the antrum were 6.02 ± 2.27 for ASB1.4- and 5.68 ± 2.81 for SS1-infected mice. The fold differences in Muc5B and Muc5AC expression in the fundus were 2.88 ± 1.63 and 3.84 ± 1.53 for ASB1.4- and SS1-infected animals, respectively.

Alterations in mucin mRNA expression were also evaluated in the duodenum. The mRNA expression levels of Muc1 were significantly increased at 4 weeks postinfection in the duodenum of *H. heilmannii*-infected mice ($P = 0.036$) and *H. pylori*-infected mice ($P = 0.047$) (see Fig. S1E in the supplemental material). Significantly increased expression of Muc5AC was seen at 4 ($P = 0.032$) and 16 ($P = 0.026$) weeks postinfection in the duodenum of *H. heilmannii*-infected mice (see Fig. S1F).

***H. heilmannii* infection stimulates Muc13 expression.** The transmembrane mucin Muc13 is not expressed in a healthy stom-

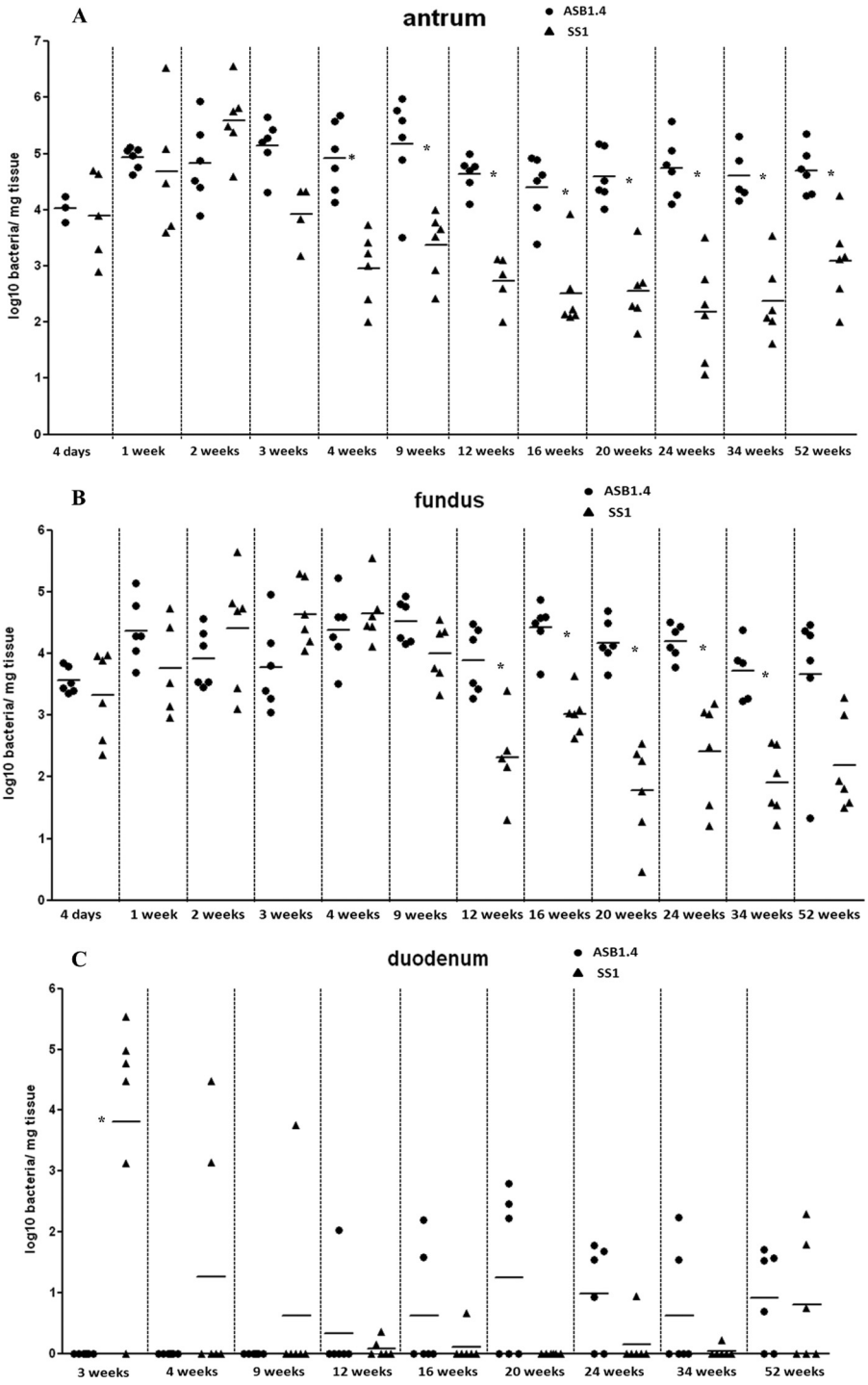

FIG 2 Colonization capacity of *H. heilmannii* ASB1.4 and *H. pylori* SS1 after experimental infection. Colonization capacity is shown as $\log_{10}$ values of bacteria per mg tissue, detected with quantitative RT-PCR in the antrum (A) and the fundus (B) of the stomach and in the duodenum (C). Animals in which no *Helicobacter* DNA could be detected in the gastrointestinal tract were set as 0. Results for individual animals are depicted by symbols around the means (lines). Statistically significant differences between animals infected with *H. heilmannii* ASB1.4 and *H. pylori* SS1 are indicated (*, $P < 0.05$, Mann-Whitney *U* test).

ach. Under healthy conditions, this cell surface mucin is mainly expressed in the glycocalyx of enterocytes and goblet cells in the small and large intestine, particularly at the luminal surface (21). Interestingly, the mRNA expression of Muc13 was significantly increased from day 1 until 9 weeks postinfection ($P < 0.001$) in the fundus of the stomach of both *H. heilmannii*- and *H. pylori*-infected mice compared to its mRNA expression in the control group (fold change for ASB1, 6.08 ± 0.84, and for SS1, 5.91 ± 1.21) (Fig. 5B; see also Fig. 2B in the supplemental material). Its mRNA expression levels were also high in the antrum (fold change

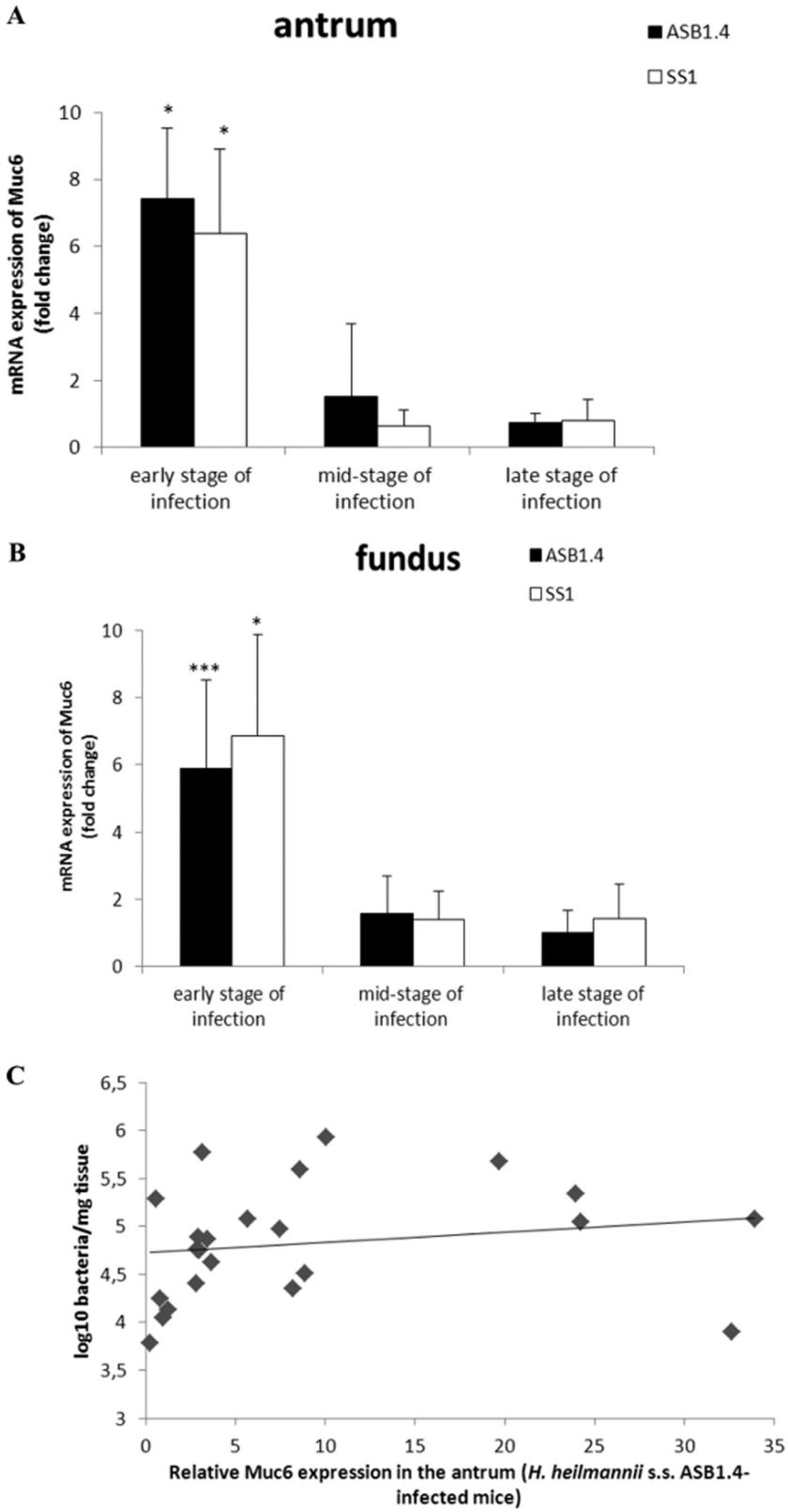

FIG 3 Muc6 expression in the stomach of *Helicobacter*-infected and control mice. Expression levels of Muc6 in the antrum (A) and fundus (B) of the stomach of ASB1.4- and SS1-infected BALB/c mice are shown. Data are presented as fold changes in gene expression normalized to 3 reference genes and relative to the results for the negative-control group, which are set as 1. Data obtained from the time points 1 day, 4 days, and 1, 2, 3, 4, and 9 weeks are pooled and designated "early stage of infection." Data obtained from the time points 12, 16, 20, and 24 weeks are pooled and designated "mid-stage of infection." Data obtained from the time points 34 and 52 weeks are pooled and designated "late stage of infection." Data are shown as means + standard deviations. Significant differences in

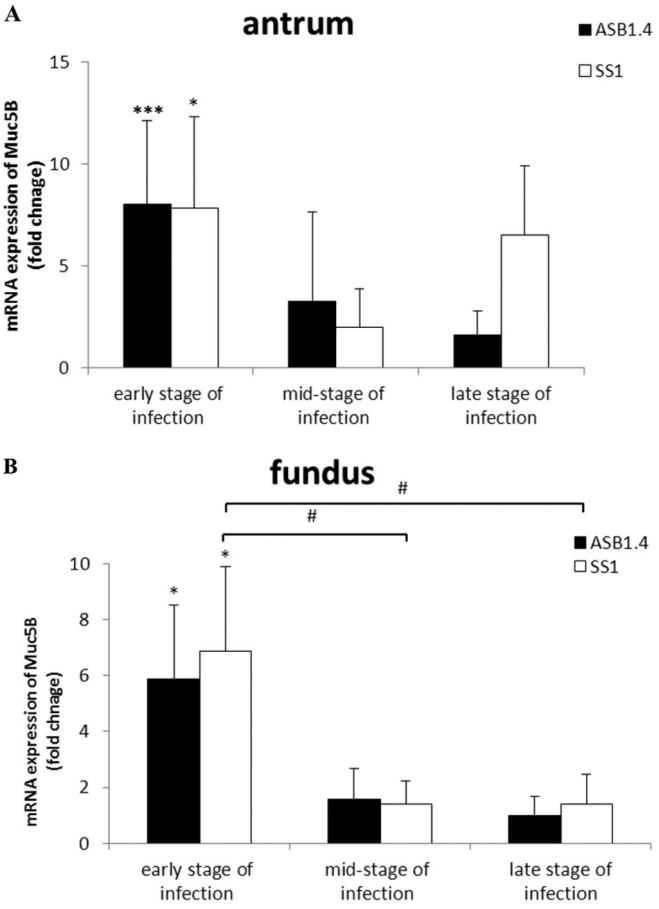

FIG 4 Muc5B expression in the stomach of *Helicobacter*-infected and control mice. Expression of Muc5B in the antrum (A) and fundus (B) of the stomach of ASB1.4- and SS1-infected BALB/c mice is shown. Data are presented as fold changes in gene expression normalized to 3 reference genes and relative to the results for the negative-control group, which are set as 1. Data obtained from the time points 1 day, 4 days, and 1, 2, 3, 4, and 9 weeks are pooled and designated "early stage of infection." Data obtained from the time points 12, 16, 20, and 24 weeks are pooled and designated "mid-stage of infection." Data obtained from the time points 34 and 52 weeks are pooled and designated "late stage of infection." Data are shown as means + standard deviations. Significant differences in expression levels between the infected groups and the negative-control group in a certain time frame (ANOVA) are indicated (*, $P < 0.05$; ***, $P < 0.001$). Significant differences in expression levels between groups inoculated with *H. heilmannii* ASB1 or *H. pylori* SS1 in different time frames (ANOVA) are indicated (#, $P < 0.05$; ###, $P < 0.001$).

for ASB1.4, 9.61 ± 4.08, and for SS1, 10.09 ± 4.38) and fundus (fold change for ASB1.4, 5.77 ± 4.33, and for SS1, 7.17 ± 3.67) of the stomach in the late stage of infection (Fig. 5A and B; see Fig. S2A and B). A significant positive correlation was observed between Muc13 expression and *Helicobacter* colonization in the fundus of *H. heilmannii*- and *H. pylori*-infected mice in the first 9 weeks postinfection (Fig. 5C and D). Although *H. heilmannii* DNA could not be found in the duodenum during the first weeks of infection, the Muc13 expression levels were significantly increased here also at 1 (fold change of 8.67 ± 1.89; $P < 0.001$) and 2 (fold change of 6.97 ± 3.09; $P < 0.001$) weeks postinfection (see Fig. S2C).

Immunohistochemical staining showed apical membrane and cytoplasmic Muc13 staining (brown) in mucus-secreting epithelial cells of the stomach of *Helicobacter*-infected mice but not in the noninfected controls (Fig. 5E and F).

***H. heilmannii* induces reduced expression of markers for gastric acid secretion by parietal cells in the fundus of the stomach.** To determine whether *Helicobacter* colonization has an impact on gastric acid secretion, the expression of different markers was analyzed (22). Quantitative RT-PCR analysis showed clear downregulation in the expression of H^+/K^+-ATPase α and β proton pump subunits in the fundus of *H. heilmannii*- and *H. pylori*-infected mice at 52 weeks postinfection (Fig. 6A and B). Compared to the control animals, whose mRNA expression levels were set to 1, the mean relative expression levels of H^+/K^+-ATPase α were 0.24 ± 0.14 and 0.2 ± 0.07 for ASB1.4- and SS1-infected animals, respectively. The H^+/K^+-ATPase β relative mean expression levels were 0.23 ± 0.15 and 0.22 ± 0.14 for ASB1.4- and SS1-infected animals, respectively. The KCNQ1 potassium channel, which colocalizes with the proton pump at the apical membrane, has been proposed to be responsible for K^+ conductance associated with acid secretion (23). Its expression levels were normal until 34 weeks postinfection but were significantly downregulated (fold change for ASB1.4, 0.2 ± 0.11, and for SS1, 0.23 ± 0.07) at 52 weeks postinfection in the fundus of *Helicobacter*-infected mice compared to its expression levels in the control group (Fig. 6C). The reductions in the fundic expression of H^+/K^+-ATPase α and β proton pump subunits and the KCNQ1 potassium channel suggest reduced gastric acid secretion by parietal cells. A loss of parietal cells could be clearly visualized by immunohistochemical staining in the fundus, close to the forestomach/stomach transition zone of the stomach of ASB1.4- and SS1-infected mice (Fig. 6D, E, and F). Quantification of parietal cells in 5 randomly chosen high-power fields in the fundus of the stomach of animals infected for 52 weeks also showed a clear reduction of parietal cells in ASB1.4- and SS1-infected mice compared to results for the controls (Fig. 6G).

Markers for metaplastic progression are upregulated in the fundus of the stomach in response to chronic infection with *H. heilmannii*. The loss of parietal cells can lead to mucous metaplasia. To investigate whether metaplastic lineages were found in the stomach, the mRNA expression of different markers for metaplastic progression was analyzed (6). From 16 weeks postinfection onwards, Muc4 expression was upregulated in the fundus of the stomach of *Helicobacter*-infected animals compared to its expression in the controls, and its expression remained high until the end of the study at 52 weeks postinfection (Fig. 7A). The mRNA expression level of Dmbt1, which has a function in epithelial cell differentiation and gastric mucosal protection (24), was highly increased between 20 and 52 weeks postinfection in the fundus of *H. heilmannii*- and *H. pylori*-infected mice (Fig. 7B). Similar results were found for the polymeric immunoglobulin receptor (pIgR), which is involved in the transport of immunoglobulin A across mucosal membranes, from the basolateral aspect of epithe-

expression levels between the infected groups and the negative-control group in a certain time frame (ANOVA) are indicated (*, $P < 0.05$; ***, $P < 0.001$). (C) Correlation analysis between Muc6 mRNA expression and the number of colonizing *Helicobacter* bacteria in the stomach of BALB/c mice. Time points 4 days, 1 week, 2, 4 and 9 weeks were taken into account. Correlation was measured by Spearman's Rho (ρ).

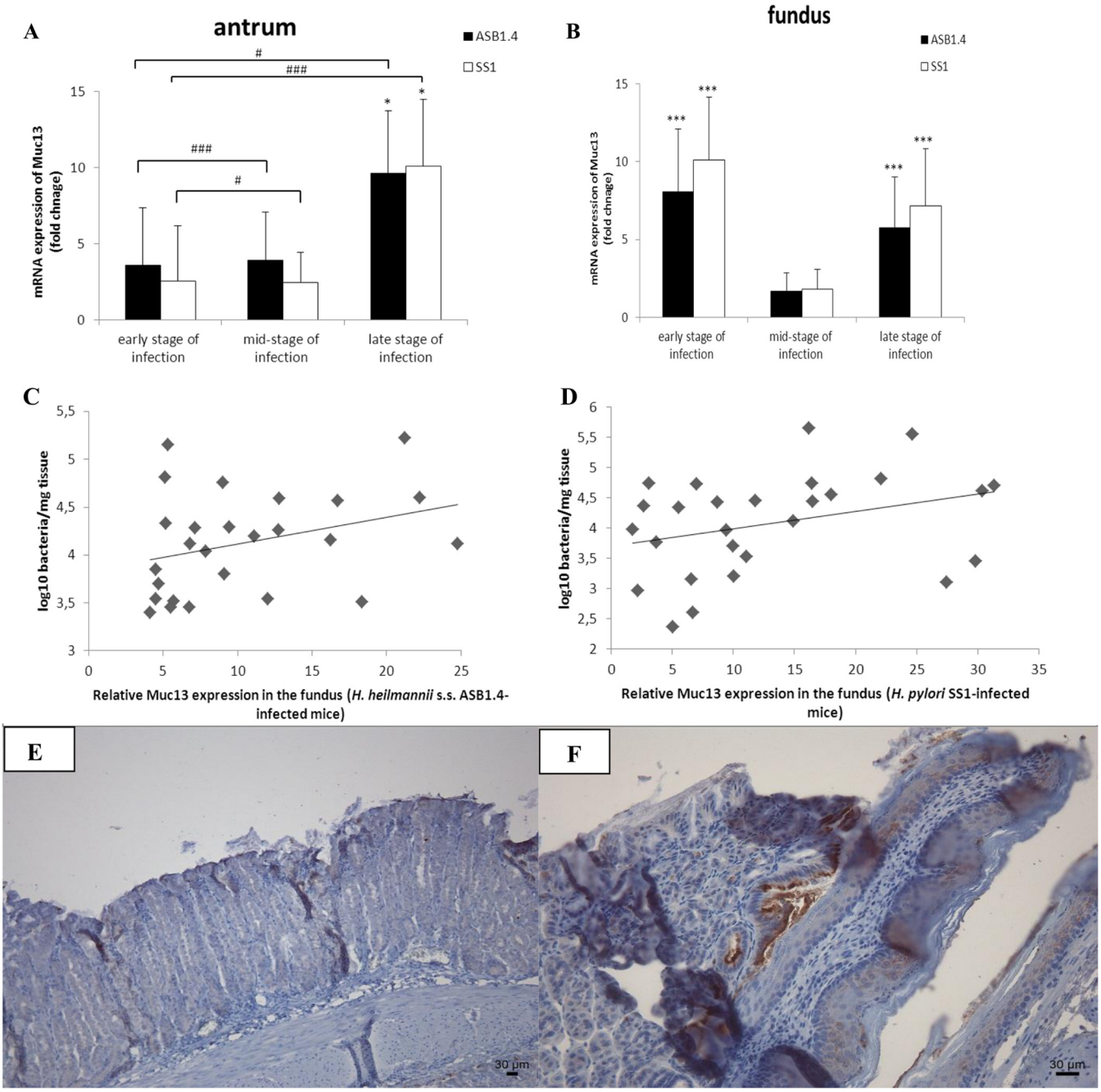

FIG 5 Muc13 expression in the stomach of *Helicobacter*-infected and control mice. Expression of Muc13 in the antrum (A) and fundus (B) of the stomach of ASB1.4- and SS1-infected BALB/c mice is shown. Data are presented as fold changes in gene expression normalized to 3 reference genes and relative to the results for the negative-control group, which are set as 1. Data obtained from the time points 1 day, 4 days, and 1, 2, 3, 4, and 9 weeks are pooled and designated "early stage of infection." Data obtained from the time points 12, 16, 20, and 24 weeks are pooled and designated "mid-stage of infection." Data obtained from the time points 34 and 52 weeks are pooled and designated "late stage of infection." Data are shown as means + standard deviations. Significant differences in expression levels between the infected groups and the negative-control group in a certain time frame (ANOVA) are indicated (*, $P < 0.05$; ***, $P < 0.001$). Significant differences in expression levels between groups inoculated with *H. heilmannii* ASB1 or *H. pylori* SS1 in different time frames (ANOVA) are indicated (#, $P < 0.05$; ###, $P < 0.001$). (C and D) Correlation analysis between Muc13 mRNA expression and the number of colonizing *Helicobacter* bacteria in the stomach of BALB/c mice. The time points 4 days and 1, 2, 4, and 9 weeks were taken into account. Correlation was measured by Spearman's Rho (ρ). (E and F) Immunohistochemical analysis of Muc13 expression (brown) in the fundus of the stomach of a control mouse (bar = 30 μm) (E) and a mouse infected with *H. heilmannii* ASB1.4 for 4 weeks (bar = 30 μm) (F).

lial cells to the luminal surface. pIgR is highly expressed in intestinal epithelial cells but is not present in the normal gastric mucosa (25). During this *in vivo* experiment, its expression level was highly upregulated from 20 weeks postinfection onwards in the fundus of mice infected with both species (Fig. 7C). The expression of Tff2 was significantly increased at 52 weeks postinfection in the fundus (fold change for ASB1.4, 6.49 ± 3.32, and for SS1, 3.44 ± 1.49) (see Fig. S3 in the supplemental material). Muc4,

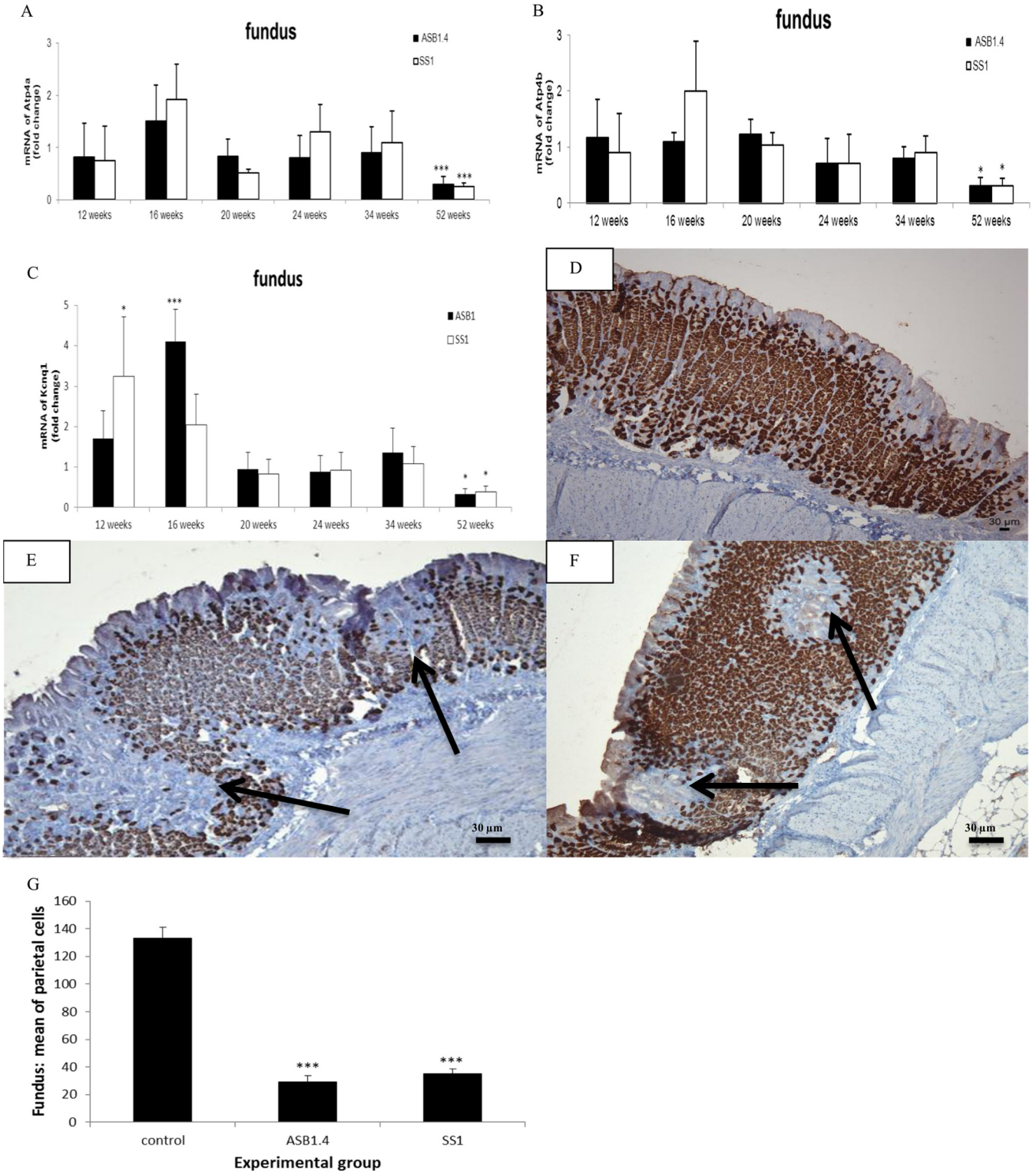

FIG 6 Analysis of parietal cells in the fundus of the stomach of *Helicobacter*-infected and control mice. (A to C) Expression levels of Atp4a (A), Atp4b (B), and Kcnq1 (C) in the fundus of the stomach of *H. heilmannii* ASB1.4- and *H. pylori* SS1-infected mice are shown. Data are presented as fold changes in gene expression normalized to 3 reference genes and relative to the results for the negative-control group, which are set as 1. Significant differences in expression levels between the infected groups and the negative-control group at a certain time point (ANOVA) are indicated (*, $P < 0.05$; ***, $P < 0.001$). (D to F) Immunohistochemical staining for the hydrogen potassium ATPase. (D) ATPase staining of the fundus of a sham-inoculated mouse. (E and F) Loss of parietal cells (arrows) was seen in the fundus of the stomach of a mouse infected with *H. heilmannii* ASB1.4 for 52 weeks (bar = 30 μm). (G) The mean numbers of parietal cells in the fundus of the stomach from mice infected with *Helicobacter* for 52 weeks and control mice are shown. The number of parietal cells in each stomach was determined by counting ATPase-positive cells in 5 randomly chosen high-power fields at the level of the gastric pits. Significant differences between *Helicobacter*-infected and control animals (ANOVA) are indicated (***, $P < 0.001$).

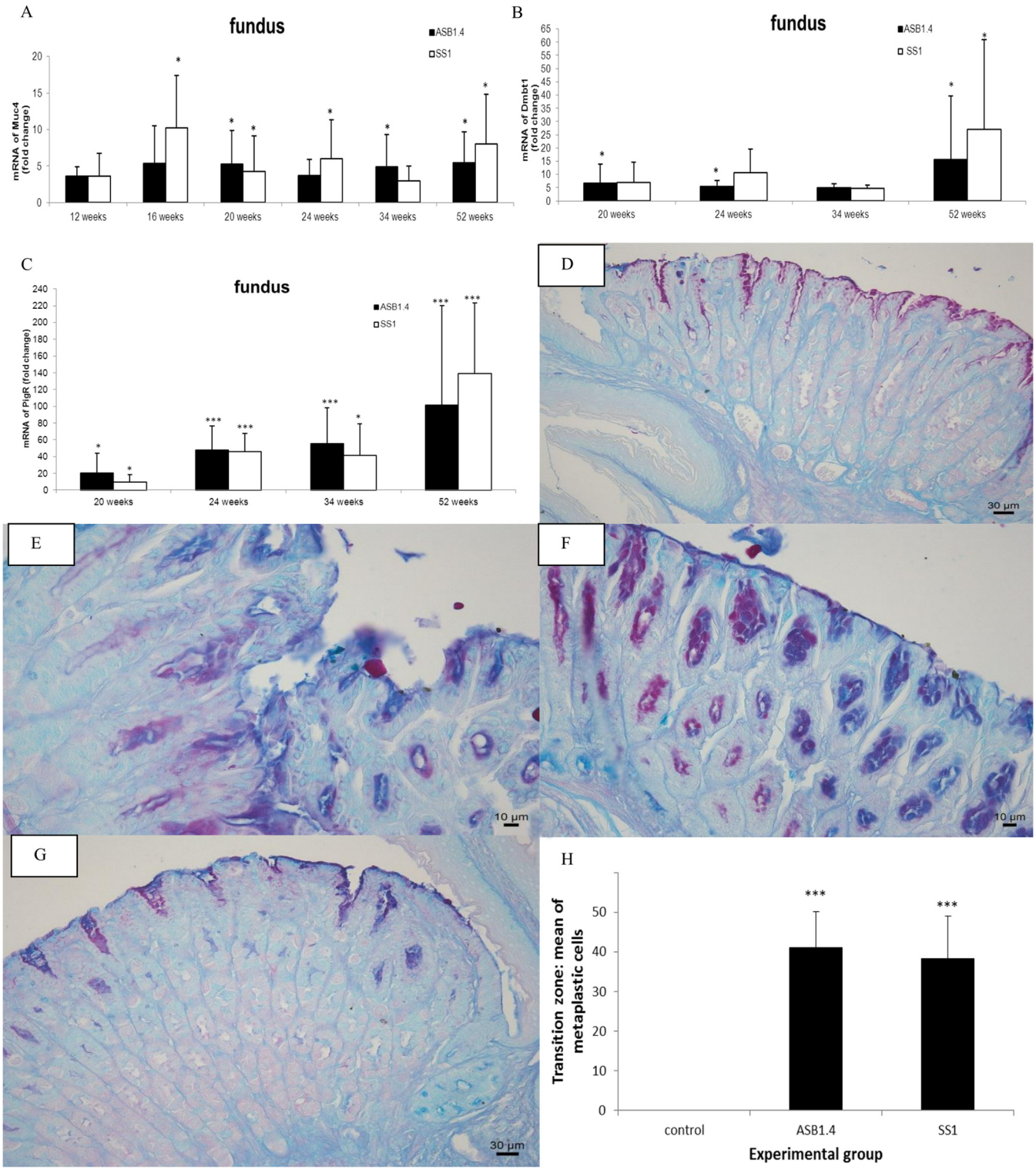

FIG 7 Determination of mucous metaplasia in the fundus of the stomach of *Helicobacter*-infected mice. (A to C) mRNA expression levels of Muc4 (A), Dmbt1 (B), and pIgR (C) in the fundus of the stomach of *H. heilmannii* ASB1.4- and *H. pylori* SS1-infected mice are shown. Data are presented as fold changes in gene expression normalized to 3 reference genes and relative to the results for the negative-control group, which are set as 1. Data are shown as means + standard deviations. Significant differences in expression level between the infected groups and the negative-control group at a certain time point (ANOVA) are indicated (*, $P < 0.05$; ***, $P < 0.001$). (D) PAS-Alcian blue staining of the forestomach/stomach transition zone of a sham-inoculated mouse (bar = 30 μm). (E and F) PAS-Alcian blue staining of the antrum (E) and the fundus (F) of the stomach of a mouse infected with *H. heilmannii* ASB1 for 24 weeks (bars = 10 μm). (G) PAS-Alcian blue staining of the forestomach/stomach transition zone of a mouse infected with *H. heilmannii* ASB1 for 52 weeks (bar = 30 μm). (E to G) Metaplastic columnar cells, mainly initiating from the transition zone junction between the forestomach and glandular epithelium along the lesser curvature (G) and, to a lesser extent, in the antrum (E) and fundus (F) of the stomach of *Helicobacter*-infected mice are indicated in blue. (H) The mean numbers of

Dmbt1, pIgR, and Tff2 have been described to be related to SPEM with chronic inflammation (6, 26). PAS-Alcian blue staining at 34 and 52 weeks postinfection showed evidence for mucous metaplasia, with metaplastic columnar glands mainly initiating from the transition zone junction between the forestomach and glandular epithelium along the lesser curvature (Fig. 7G) and, to a lesser extent, in the antrum (Fig. 7E) and fundus (Fig. 7F) of the stomach of *Helicobacter*-infected mice. Quantification of blue-stained metaplastic cells in 5 randomly chosen high-power fields in the forestomach/stomach transition zone also highlighted the presence of mucous metaplasia in the stomach of animals infected for 52 weeks with ASB1.4 and SS1 but not in the noninfected controls (Fig. 7H).

DISCUSSION

In BALB/c mice infected with *H. heilmannii* ASB1.4 and *H. pylori* SS1 for 52 weeks, MALT lymphoma-like lesions were observed in a narrow zone in the fundus near the forestomach/stomach transition zone. These pathological lesions might eventually lead to gastric MALT lymphoma (12). The risk of developing MALT lymphoma has been suggested to be higher in humans suffering from an NHPH gastritis than in those infected with *H. pylori* (15). Gastric MALT lymphoma is characterized by a strong proliferation of B-lymphocytes, which may be dependent on Th2-type cytokines (15, 16). Experimental NHPH infections have indeed been shown to evoke a Th2-polarized response (14, 16), suggesting that Th2-prone BALB/c mice (27) infected with NHPH can be seen as a critical model for the development of MALT lymphoma induced by NHPH.

It has been demonstrated that *H. pylori* strains mainly stimulate Th1 responses both in humans and in mouse models (28). However, as an exception, the *H. pylori* strain SS1 does not cause a significant upregulation of gamma interferon (IFN-γ), a signature Th1 marker, in either BALB/c or C57BL/6 mice. Nevertheless, in common with other NHPH, it elicits a Th2 response in mice (17, 29). This may explain the development of MALT lymphoma-like lesions in the stomach seen in this and other studies (29). Typical for *H. pylori* strains inducing MALT lymphoma is that they lack genes encoding major virulence factors, such as a functional CagPAI, Bab, and Sab adhesins (30). *H. pylori* SS1 indeed lacks a functional CagPAI (17). This strain also does not bind to the glycan structures Le^b and sLe^x that are expressed by human gastric mucins (1, 3; also unpublished data). Binding to Le^b and sLe^x has been shown to be mediated by the *H. pylori* BabA and SabA adhesins, respectively (1, 3), suggesting that SS1 does not express these adhesins. These virulence factors, as well as a functional CagPAI, are also absent in *H. heilmannii* and other NHPH (31–34).

In this study, *H. heilmannii* ASB1.4 and *H. pylori* SS1 colonized both the antrum and fundus of the stomach but with a higher colonization density in the antrum. This is similar to what has been described in human patients. Indeed, in humans infected with NHPH, colonization mainly occurs in the antrum of the stomach but these bacteria may be found in the fundus as well, which has also been described for *H. pylori* (10). In the present study, *H. heilmannii*-infected BALB/c mice showed higher colonization rates in the antrum and fundus of the stomach than *H. pylori*-infected mice. This indicates that the capacity of ASB1.4 to persist in the stomach of BALB/c mice is higher than that of SS1, which showed a reduction in colonization during the later stages of infection. The latter finding has also been reported by Schmitz et al. (20). DNA from *H. heilmannii* ASB1.4 and *H. pylori* SS1 was also found in the duodenum. Since both species have been linked to duodenal ulcer disease (10), it remains to be elucidated whether they are able to colonize the duodenum or whether the quantitative RT-PCR just picked up DNA from bacteria colonizing the stomach.

The expression of MUC1, MUC5AC, and MUC6 in the human gastric epithelium in relation to *H. pylori* colonization has been investigated previously, showing that *H. pylori* interacts with epithelial cells that produce MUC1 and MUC5AC by binding to Le^b and sLe^x expressed by these mucins. This indicated that MUC1 and MUC5AC but not MUC6 play a role in the colonization of *H. pylori* in the gastric mucosa (1, 3). On the contrary, in this study, a clear upregulation of Muc6 but not Muc5AC and Muc1 was seen in the stomach of *H. heilmannii* ASB1.4-infected BALB/c mice in the first 9 weeks postinfection. The pathway regulating gastric MUC6 expression in response to *H. heilmannii* infection in the human stomach, as well as the bacterial factors involved, is unknown and needs further investigation. During this early stage of infection, the increased expression of Muc6 in the antrum was also positively correlated with the number of *H. heilmannii* bacteria. Since Muc6 is expressed by the glands and, unlike *H. pylori* (1), NHPH are mainly localized in the deep glands of the gastric mucosa (10, 15, 16), a potential role of Muc6 in *H. heilmannii* colonization is suggested and needs to be further unraveled. Whether Muc6 plays a role in the colonization of *H. pylori* strains lacking the BabA and SabA adhesins, such as the SS1 strain, also needs further investigation.

Another interesting finding seen during *H. heilmannii* ASB1.4 infection, as well as during *H. pylori* SS1 infection, was the increased mRNA expression of Muc13 in the stomach. MUC13 has been shown to be highly expressed in human gastric cancer (21), but increased mRNA expression of it in the early stages of *Helicobacter* colonization has so far never been described. The positive correlation found between the increased Muc13 expression and the increased number of *Helicobacter* bacteria in the fundus of the stomach during the first 9 weeks of infection suggests a potential role for Muc13 in *Helicobacter* colonization. The expression level of Muc13 remained upregulated until 52 weeks postinfection. It has been described that sustained elevation of the expression of cell surface mucins may promote the transition from chronic inflammation to cancer (21). How Muc13 influences the *Helicobacter* colonization process is unknown and needs further investigation.

In this study, the mRNA expression of several markers for gastric acid secretion by parietal cells was significantly reduced at 52 weeks postinfection in the fundic epithelium of *H. heilmannii*-infected mice, suggesting the loss of parietal cell function. A clear loss of parietal cells was indeed shown by immunohistochemical staining. Parietal cell loss might eventually lead to the develop-

metaplastic cells in the forestomach/stomach transition zone of the mice infected with *Helicobacter* for 52 weeks and control mice are shown. The numbers of metaplastic cells were determined by counting blue cells in 5 randomly chosen high-power fields after staining with PAS-Alcian blue. Significant differences between *Helicobacter*-infected and control animals (ANOVA) are indicated (***, $P < 0.001$).

ment of mucous metaplasia (6). Markers for metaplastic progression into SPEM were indeed found to be upregulated in the fundic region of the stomach during later stages of infection with *H. heilmannii* ASB1.4 and *H. pylori* SS1. Mucous metaplasia in a narrow zone of the fundus near the limiting ridge of the stomach of *H. heilmannii*-infected mice was histologically confirmed. MALT lymphoma-like lesions were also seen in this region. In gastric cancer, intestinal metaplasia present in the mucosa surrounding low-grade MALT lymphomas has been described (35). However, in our study, evidence for intestinal metaplasia, such as *de novo* expression of Muc2 as described in *H. pylori* infection (7), was not seen. It remains, therefore, to be determined whether SPEM may further differentiate into intestinal metaplasia and, in the worst-case scenario, into dysplasia in mice kept for longer than 1 year after experimental infection with *H. heilmannii*.

Taken together, the results of histopathology and quantitative RT-PCR in the present experimental infection study in BALB/c mice illustrate that infection with *H. heilmannii* induced severe gastric pathology that progressed into MALT lymphoma-like lesions and SPEM, as well as inducing changes in the expression of Muc6 and Muc13 in the stomach.

ACKNOWLEDGMENTS

This work was supported by the Research Fund of Ghent University, Belgium, grant GOA 01G00408 and grant 01SC0312, the China Scholarship Council (CSC) (grant 2011691031), the Swedish Research Council (Vetenskapsrådet 521-2011 to 2370), and the Swedish Cancer Foundation (Cancerfonden).

We are grateful to Nathalie Van Rysselberghe, Sofie De Bruyckere, Christian Puttevils, and Sarah Loomans for their skillful technical assistance.

REFERENCES

1. **Lindén SK, Nordman H, Hedenbro J, Hurtig M, Borén T, Carlstedt I.** 2002. Strain- and blood group-dependent binding of *Helicobacter pylori* to human gastric MUC5AC glycoforms. Gastroenterology **123:**1923–1930. http://dx.doi.org/10.1053/gast.2002.37076.
2. **McGuckin MA, Lindén SK, Sutton P, Florin TH.** 2011. Mucin dynamics and enteric pathogens. Nat. Rev. Microbiol. **9:**265–278. http://dx.doi.org/10.1038/nrmicro2538.
3. **Lindén SK, Sheng YH, Every AL, Miles KM, Skoog EC, Florin TH, Sutton P, McGuckin MA.** 2009. MUC1 limits *Helicobacter pylori* infection both by steric hindrance and by acting as a releasable decoy. PLoS Pathog. **5:**e1000617. http://dx.doi.org/10.1371/journal.ppat.1000617.
4. **Taupin D, Podolsky DK.** 2003. Trefoil factors: initiators of mucosal healing. Nat. Rev. Mol. Cell Biol. **4:**721–732. http://dx.doi.org/10.1038/nrm1203.
5. **Skoog EC, Sjöling Å, Navabi N, Holgersson J, Lundin SB, Lindén SK.** 2012. Human gastric mucins differently regulate *Helicobacter pylori* proliferation, gene expression and interactions with host cells. PLoS One **7:**e36378. http://dx.doi.org/10.1371/journal.pone.0036378.
6. **Weis VG, Sousa JF, LaFleur BJ, Nam KT, Weis JA, Finke PE, Ameen NA, Fox JG, Goldenring JR.** 2013. Heterogeneity in mouse spasmolytic polypeptide-expressing metaplasia lineages identifies markers of metaplastic progression. Gut **62:**1270–1279. http://dx.doi.org/10.1136/gutjnl-2012-302401.
7. **Mejías-Luque R, Lindén SK, Garrido M, Tye H, Najdovska M, Jenkins BJ, Iglesias M, Ernst M, de Bolós C.** 2010. Inflammation modulates the expression of the intestinal mucins MUC2 and MUC4 in gastric tumors. Oncogene **29:**1753–1762. http://dx.doi.org/10.1038/onc.2009.467.
8. **Reis CA, David L, Correa P, Carneiro F, de Bolós C, Garcia E, Mandel U, Clausen H, Sobrinho-Simões M.** 1999. Intestinal metaplasia of human stomach displays distinct patterns of mucin (MUC1,MUC2, MUC5AC,and MUC6) expression. Cancer Res. **59:**1003–1007.
9. **Shimamura T, Ito H, Shibahara J, Watanabe A, Hippo Y, Taniguchi H, Chen Y, Kashima T, Ohtomo T, Tanioka F, Iwanari H, Kodama T, Kazui T, Sugimura H, Fukayama M, Aburatani H.** 2005. Over expression of MUC13 is associated with intestinal-type gastric cancer. Cancer Sci. **96:**265–273. http://dx.doi.org/10.1111/j.1349-7006.2005.00043.x.
10. **Haesebrouck F, Pasmans F, Flahou B, Chiers K, Baele M, Meyns T, Decostere A, Ducatelle R.** 2009. Gastric helicobacters in domestic animals and nonhuman primates and their significance for human health. Clin. Microbiol. Rev. **22:**202–223. http://dx.doi.org/10.1128/CMR.00041-08.
11. **Smet A, Flahou B, D'Herde K, Vandamme P, Cleenwerck I, Ducatelle R, Pasmans F, Haesebrouck F.** 2012. *Helicobacter heilmannii* sp. nov., isolated from feline gastric mucosa. Int. J. Syst. Evol. Microbiol. **62:**299–306. http://dx.doi.org/10.1099/ijs.0.029207-0.
12. **O'Rourke JL, Dixon MF, Jack A, Enno A, Lee A.** 2004. Gastric B-cell mucosa-associated lymphoid tissue (MALT) lymphoma in an animal model of '*Helicobacter heilmannii*' infection. J. Pathol. **203:**896–903. http://dx.doi.org/10.1002/path.1593.
13. **Smet A, Van Nieuwerburgh F, Ledesma J, Flahou B, Deforce D, Ducatelle R, Haesebrouck F.** 2013. Genome sequence of *Helicobacter heilmannii* sensu stricto ASB1 isolated from the gastric mucosa of a kitten with severe gastritis. Genome Announc. **1:**e00033–12. http://dx.doi.org/10.1128/genomeA.00033-12.
14. **Joosten M, Blaecher C, Flahou B, Ducatelle R, Haesebrouck F, Smet A.** 2013. Diversity in bacterium-host interactions within the species *Helicobacter heilmannii* sensu stricto. Vet. Res. **44:**65. http://dx.doi.org/10.1186/1297-9716-44-65.
15. **Flahou B, Haesebrouck F, Pasmans F, D'Herde K, Driessen A, Van Deun K, Smet A, Duchateau L, Chiers K, Ducatelle R.** 2010. *Helicobacter suis* causes severe gastric pathology in mouse and Mongolian gerbil models of human gastric disease. PLoS One **5:**e14083. http://dx.doi.org/10.1371/journal.pone.0014083.
16. **Flahou B, Van Deun K, Pasmans F, Smet A, Volf J, Rychlik I, Ducatelle R, Haesebrouck F.** 2012. The local immune response of mice after *Helicobacter suis* infection: strain differences and distinction with *Helicobacter pylori*. Vet. Res. **43:**75. http://dx.doi.org/10.1186/1297-9716-43-75.
17. **Crabtree JE, Ferrero RL, Kusters JG.** 2002. The mouse colonizing *Helicobacter pylori* strain SS1 may lack a functional cag pathogenicity island. Helicobacter **7:**139–140. http://dx.doi.org/10.1046/j.1083-4389.2002.00071.x.
18. **O'Rourke JL, Solnick JV, Neilan BA, Seidel K, Hayter R, Hansen LM, Lee A.** 2004. Description of "*Candidatus* Helicobacter heilmannii" based on DNA sequence analysis of 16S rRNA and urease genes. Int. J. Syst. Evol. Microbiol. **54:**2203–2211. http://dx.doi.org/10.1099/ijs.0.63117-0.
19. **Livak KJ, Schmittgen TD.** 2001. Analysis of relative gene expression data using real-time quantitative PCR and the $2^{-\Delta\Delta CT}$ method. Methods **25:**402–408. http://dx.doi.org/10.1006/meth.2001.1262.
20. **Schmitz JM, Durham CG, Ho SB, Lorenz RG.** 2009. Gastric mucus alterations associated with murine *Helicobacter* infection. J. Histochem. Cytochem. **57:**457–467. http://dx.doi.org/10.1369/jhc.2009.952473.
21. **Sheng YH, Lourie R, Lindén SK, Jeffery PL, Roche D, Tran TV, Png CW, Waterhouse N, Sutton P, Florin TH, McGuckin MA.** 2011. The MUC13 cell-surface mucin protects against intestinal inflammation by inhibiting epithelial cell apoptosis. Gut **60:**1661–1670. http://dx.doi.org/10.1136/gut.2011.239194.
22. **Jain RN, Brunkan CS, Chew CS, Samuelson LC.** 2006. Gene expression profiling of gastrin target genes in parietal cells. Physiol. Genomics **24:**124–132. http://dx.doi.org/10.1152/physiolgenomics.00133.2005.
23. **Grahammer F, Herling AW, Lang HJ, Schmitt-Gräff A, Wittekindt OH, Nitschke R, Bleich M, Barhanin J, Warth R.** 2001. The cardiac K+ channel KCNQ1 is essential for gastric acid secretion. Gastroenterology **120:**1363–1371. http://dx.doi.org/10.1053/gast.2001.24053.
24. **Conde AR, Martins AP, Brito M, Manuel A, Ramos S, Malta-Vacas J, Renner M, Poustka A, Mollenhauer J, Monteiro C.** 2007. DMBT1 is frequently downregulated in well-differentiated gastric carcinoma but more frequently upregulated across various gastric cancer types. Int. J. Oncol. **30:**1441–1446.
25. **Gologan A, Acquafondata M, Dhir R, Sepulveda AR.** 2008. Polymeric immunoglobulin receptor-negative tumors represent a more aggressive type of adenocarcinomas of distal esophagus and gastroesophageal junction. Arch. Pathol. Lab. Med. **132:**1295–1301.
26. **Nomura S, Baxter T, Yamaguchi H, Leys C, Vartapetian AB, Fox JG, Lee JR, Wang TC, Goldenring JR.** 2004. Spasmolytic polypeptide expressing metaplasia to preneoplasia in *H. felis*-infected mice. Gastroenterology **127:**582–594. http://dx.doi.org/10.1053/j.gastro.2004.05.029.
27. **Enno A, O'Rourke J, Braye S, Howlett R, Lee A.** 1998. Antigen-dependent

progression of mucosa-associated lymphoid tissue (MALT)-type lymphoma in the stomach. Effects of antimicrobial therapy on gastric MALT lymphoma in mice. Am. J. Pathol. **152:**1625–1632.

28. **Robinson K, Loughlin MF, Potter R, Jenks PJ.** 2005. Host adaptation and immune modulation are mediated by homologous recombination in *Helicobacter pylori*. J. Infect. Dis. **191:**579–587. http://dx.doi.org/10.1086/427657.
29. **Thompson LJ, Danon SJ, Wilson JE, O'Rourke JL, Salama NR, Falkow S, Mitchell H, Lee A.** 2004. Chronic *Helicobacter pylori* infection with Sydney strain 1 and a newly identified mouse-adapted strain (Sydney strain 2000) in C57BL/6 and BALB/c mice. Infect. Immun. **72:**4668–4679. http://dx.doi.org/10.1128/IAI.72.8.4668-4679.2004.
30. **Thiberge JM, Boursaux-Eude C, Lehours P, Dillies MA, Creno S, Coppée JY, Rouy Z, Lajus A, Ma L, Burucoa C, Ruskoné-Foumestraux A, Courillon-Mallet A, De Reuse H, Boneca IG, Lamarque D, Mégraud F, Delchier JC, Médigue C, Bouchier C, Labigne A, Raymond J.** 2010. From array-based hybridization of *Helicobacter pylori* isolates to the complete genome sequence of an isolate associated with MALT lymphoma. BMC Genomics **11:**368. http://dx.doi.org/10.1186/1471-2164-11-368.
31. **Smet A, Van Nieuwerburgh F, Ledesma J, Flahou B, Deforce D, Ducatelle R, Haesebrouck F.** 2013. Genome sequence of *Helicobacter heilmannii sensu stricto* ASB1 isolated from the gastric mucosa of a kitten with severe gastritis. Genome Announc. **1:**e00033–12. http://dx.doi.org/10.1128/genomeA.00033-12.
32. **Vermoote M, Vandekerckhove TT, Flahou B, Pasmans F, Smet A, De Groote D, Van Criekinge W, Ducatelle R, Haesebrouck F.** 2011. Genome sequence of *Helicobacter suis* supports its role in gastric pathology. Vet. Res. **42:**51. http://dx.doi.org/10.1186/1297-9716-42-51.
33. **Schott T, Kondadi PK, Hänninen ML, Rossi M.** 2011. Comparative genomics of *Helicobacter pylori* and the human-derived *Helicobacter bizzozeronii* CIII-1 strain reveal the molecular basis of the zoonotic nature of non-*pylori* gastric *Helicobacter* infections in humans. BMC Genomics **12:**534. http://dx.doi.org/10.1186/1471-2164-12-534.
34. **Arnold IC, Zigova Z, Holden M, Lawley TD, Rad R, Dougan G, Falkow S, Bentley SD, Müller A.** 2011. Comparative whole genome sequence analysis of the carcinogenic model pathogen *Helicobacter felis*. Genome Biol. Evol. **3:**302–308. http://dx.doi.org/10.1093/gbe/evr022.
35. **Lamarque D, Levy M, Chaumette MT, Roudot-Thoraval F, Cavicchi M, Auroux J, Courillon-Mallet A, Haioun C, Delchier JC.** 2006. Frequent and rapid progression of atrophy and intestinal metaplasia in gastric mucosa of patients with MALT lymphoma. Am. J. Gastroenterol. **101:**1886–1893. http://dx.doi.org/10.1111/j.1572-0241.2006.00671.x.